Metabolic Engineering 94 (2026) 45–56

Contents lists available at ScienceDirect

Metabolic Engineering

journal homepage: www.elsevier.com/locate/meteng

Disruption of acyl-acyl carrier protein (acyl-ACP) synthetase in cyanobacteria impairs lipid remodeling as revealed by acyl-ACP measurements

Juthamas Jaroensuk [a,*], Joshua P. Abraham [b], Baltazar E. Zuniga [c], Hawkins S. Shepard [d], Michael Wei [a], Russell Williams [a], Stewart A. Morley [a], Maneesh Lingwan [a], Jiahong Zhou [a], Michael A. Jindra [b,1], Poonam Jyoti [a,2], Bo Wang [e,3], Jody C. May [d], John A. McLean [d], Jamey D. Young [c,e], Brian F. Pfleger [b], Doug K. Allen [a,**]

[a] Donald Danforth Plant Science Center, St. Louis, MO, USA
[b] Chemical and Biological Engineering, University of Wisconsin, Madison, WI, USA
[c] Molecular Physiology and Biophysics, Vanderbilt University, Nashville, TN, USA
[d] Chemistry, Vanderbilt University, Nashville, TN, USA
[e] Chemical and Biomolecular Engineering, Vanderbilt University, Nashville, TN, USA

ARTICLE INFO

Keywords:
Fatty acid synthesis
Systems biology
Lipid remodeling
Cyanobacteria
Biofuel
Acyl-ACP synthetase

ABSTRACT

Free fatty acid (FFA) production in bacteria is a key target for metabolic engineering. The knockout of the acyl-ACP synthetase (AAS) prevents reincorporation of FFA into the fatty acid biosynthetic cycle and is widely used to enhance their secretion. However, the role of AAS in membrane lipid remodeling under environmental stress, such as altered temperature, remains poorly understood. In cyanobacteria, temperature shifts are known to affect fatty acid desaturation and membrane fluidity, yet it is unclear whether AAS contributes to these adaptive responses through re-esterification of membrane-released acyl chains. We elucidated unique aspects of fatty acid metabolism in response to temperature changes in biotechnologically relevant microbes with the development of an efficient method for quantifying acyl-ACP intermediates using anion exchange chromatography (AEX). In *Escherichia coli,* which performs desaturation during fatty acid biosynthesis, we detected saturated and unsaturated acyl-ACPs that confirm biosynthetic pathway operation. In the cyanobacteria, *Picosynechococcus* sp. PCC 7002 and the Δ*aas* strain, changes between two temperatures were interpreted with support from proteomic and lipidomic analyses and indicated that the AAS is tied to membrane lipid remodeling. Further, polyunsaturated acyl-ACPs were detected in the Δ*aas* strain, which was unexpected because fatty acid synthesis does not produce polyunsaturates in cyanobacteria, suggesting the presence of alternative acyl-activating enzymes or unknown acyl-ACP desaturases. This study highlights the possible link between acyl chain recycling and lipid remodeling in cyanobacteria and demonstrates the utility of AEX-based acyl-ACP profiling in dissecting fatty acid metabolism.

1. Introduction

Lipids are essential to living organisms, forming membranes that spatially define cells and organelles, functioning as signaling molecules for metabolism and in response to stress, and acting as a storage reserve that contains twice the energy of carbohydrates (Allen et al., 2015;

* Corresponding author.
** Corresponding author.
E-mail addresses: jjaroensuk@danforthcenter.org (J. Jaroensuk), dallen@danforthcenter.org (D.K. Allen).
[1] Present address: LanzaTech, 8045 Lamon Ave #400, Skokie, IL.
[2] Present address: Department of Biotech, Council of Scientific & Industrial Research (CSIR) - Institute of Himalayan Bioresource Technology (IHBT), Palampur, India.
[3] Present address: Department of Bioproducts and Biosystems Engineering, College of Food, Agricultural and Natural Resource Sciences, University of Minnesota, St. Paul, MN, USA.

https://doi.org/10.1016/j.ymben.2025.11.004
Received 17 June 2025; Received in revised form 2 November 2025; Accepted 5 November 2025
Available online 5 November 2025

Mukherjee et al., 2024; Suh et al., 2022; Yu et al., 2021; Sohlenkamp and Geiger, 2015; Li-Beisson et al., 2019; Chapman and Ohlrogge, 2012). Lipids are essential components of animal and human diets and are highly valued as eco-friendly replacement feedstocks for fuels, polymers, surfactants, and other societal needs that are predominantly derived from petroleum (Lu et al., 2011). It is estimated that by 2050, the production of lipids must double to meet global demand (Faostat, 2022). Small changes in lipid production can significantly impact the economics of crops (Mukherjee et al., 2024) that are a primary source of acyl chains for fuels and feedstocks (Yu et al., 2011a). However, microbes can grow considerably faster than plants, requiring limited space or land, and could provide a sustainable complement to plant-based products. Engineering fast-growing microbes to produce elevated levels of fatty acids and other lipids would contribute to the goal of a sustainable bioeconomy (Jaroensuk et al., 2024; Intasian et al., 2021; Jouhet et al., 2024).

Bacteria, both autotrophs (e.g., cyanobacteria) and heterotrophs (e.g., *E. coli*), utilize type II fatty acid synthesis with multiple monofunctional enzymes (White et al., 2005; Cronan and Thomas, 2009). Fatty acids are generated from the sequential condensation of acetyl groups with an acyl chain attached to an acyl carrier protein (ACP) scaffold (Chan and Vogel, 2010). Fatty acid synthesis entails four successive enzymatic reactions: condensation, reduction, dehydration, and a second reduction. The respective intermediates of these reactions are β-ketoacyl-ACP, β-hydroxyacyl-ACP, *trans-2*-enoyl-ACP, and a fully reduced acyl-ACP that is longer by two carbons (Fig. 1) (White et al., 2005; Birge and Vagelos, 1972; Cronan, 2024; Bloch, 1969; Kass et al., 1967; Cronan et al., 1969; Choi et al., 2000; Heath and Rock, 1995, 1996a, 1996b; Ruch and Vagelos, 1973; Lai and Cronan, 2004; Borgaro et al., 2011). This cycle repeats until the acyl chains reach 16 or 18 carbons in length (in most microorganisms) and are diverted to prokaryotic lipid assembly (Yu et al., 2011a; Allen, 2016). Alternatively, the acyl group can be cleaved by a thioesterase, if present, resulting in non-esterified or free fatty acids (FFA) for the production of oleochemicals.

Although the type II fatty acid synthesis pathway is common in microbes, the process of desaturation of fatty acids differs depending on the organism (Cronan, 2024; Los and Murata, 1998). In some microbes, including *E. coli*, unsaturated fatty acids are synthesized by an oxygen-independent FabA-FabB pathway, where a *cis* double bond is introduced into the acyl chain of the 10-carbon acyl-ACP intermediate (Birge and Vagelos, 1972; Bloch, 1969; Kass et al., 1967; Cronan et al., 1969; Feng and Cronan, 2009; Norris and Bloch, 1963). During this process, FabA catalyzes the dehydration of β-hydroxydecanoyl-ACP to *trans*-2-decenoyl-ACP, which is then isomerized to *cis*-3-decenoyl-ACP, serving as a starting intermediate for sequential steps involving FabB, FabG, FabZ, and FabI to produce unsaturated fatty acids in the synthesis cycle (Birge and Vagelos, 1972; Bloch, 1969; Kass et al., 1967; Cronan

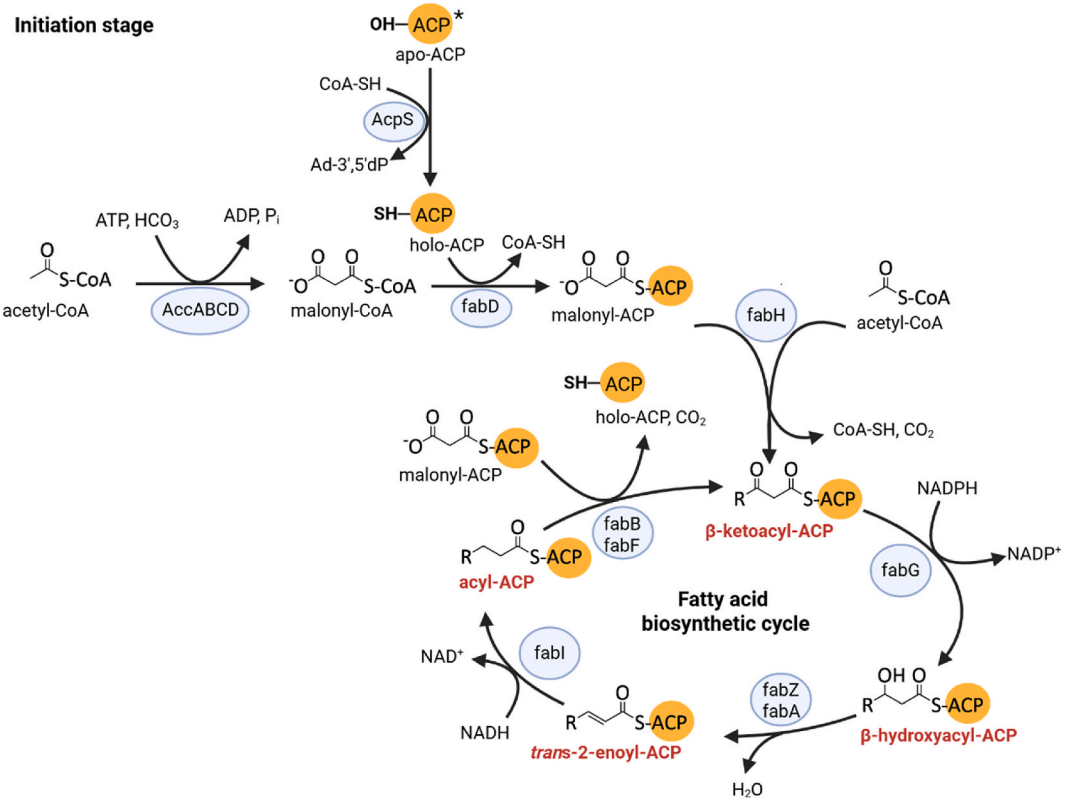

Fig. 1. Saturated fatty acid biosynthesis in microbes (White et al., 2005; Birge and Vagelos, 1972; Cronan, 2024; Bloch, 1969; Kass et al., 1967; Cronan et al., 1969; Choi et al., 2000; Heath and Rock, 1995, 1996a, 1996b; Ruch and Vagelos, 1973; Lai and Cronan, 2004; Borgaro et al., 2011). Fatty acid biosynthesis initiates with converting an apo-ACP to a holo-ACP form by ACP synthase (AcpS). The holo form includes a 4-phosphopantetheinyl arm that covalently links to fatty acid intermediates. After initiation, holo-ACP is recycled in the fatty acid biosynthetic cycle. The source of carbon for the cycle originates from acetyl-CoA, which is carboxylated by acetyl-CoA carboxylase (AccABCD) to form malonyl-CoA and then transferred to holo-ACP by s-malonyltransferase (FabD), generating malonyl-ACP, the key substrate for chain elongation and additionally producing a free CoA molecule. In fatty acid synthesis, β-ketoacyl-ACP synthase III (FabH) catalyzes the first condensation of acetyl-CoA with malonyl-ACP, producing acetoacetyl-ACP, (the initial β-ketoacyl-ACP), and CoA-SH. In subsequent synthesis cycles, β-ketoacyl-ACP synthase I enzymes (FabB/FabF) add malonyl-ACP to the growing chain. The β-ketoacyl-ACP intermediates undergo reduction by 3-oxoacyl-ACP reductase (FabG), dehydration involving β-hydroxyacyl-ACP dehydratase (FabZ/FabA), and a second reduction by an enoyl-ACP reductase (FabI) to form acyl-ACP, which is propagated through the cycle repeatedly to produce a full-length fatty acid. This Type II Fatty Acid Synthase (FAS) system enables fatty acid synthesis for membrane lipid formation and cellular metabolism. Abbreviations: Ad-3′,5′dP—adenosine 3′,5′-phosphate. Asterisk (*) indicates the apo-ACP does not contain a 4-phosphopantetheinyl arm. Created with aid from BioRender.com.

et al., 1969; Feng and Cronan, 2009; Norris and Bloch, 1963). This is distinct from cyanobacteria, where the substrate for desaturation of fatty acids is a glycerolipid (Los and Murata, 1998; Sato et al., 2009; Higashi and Murata, 1993; Wada et al., 1993a, 1993b; Effendi et al., 2023; Sakamoto et al., 1994; Starikov et al., 2022; Murata and Wada, 1995), and does not involve fatty acid synthesis cycle intermediates as in *E. coli*. Instead, cyanobacteria utilize an oxygen-dependent pathway, catalyzed by membrane-bound desaturases (Los and Murata, 1998; Sato et al., 2009; Higashi and Murata, 1993; Wada et al., 1993a, 1993b; Effendi et al., 2023; Sakamoto et al., 1994; Starikov et al., 2022; Murata and Wada, 1995; Mendez-Perez et al., 2014). Enzymes such as DesA, DesB, and DesC introduce double bonds into fatty acids already esterified to galacto-, sulfo-, and phospholipids (Murata and Wada, 1995; Murata et al., 1992; Los et al., 1997; Sakamoto and Bryant, 1997). While the regiospecificity and substrate preferences of these enzymes vary by species and remain incompletely characterized (Murata and Wada, 1995; Murata et al., 1992), they operate without a phosphatidylcholine (PC)-based acyl editing cycle, which in plants supports acyl chain desaturation and remodeling via removal and re-attachment to PC (Bates et al., 2007, 2009). Analogous mechanisms that recycle acyl chains and enhance lipid desaturation in cyanobacteria are unknown but could contribute to lipid remodeling to maintain membrane fluidity during changes in temperature (Murata and Wada, 1995; Murata et al., 1992; Sakamoto et al., 1997; Sérès et al., 2025; Douchi et al., 2023).

Independent of fatty acid biosynthesis, acyl-ACPs can be generated by acyl-ACP synthetase (AAS), which attaches a FFA to an ACP backbone. Since cyanobacteria lack beta oxidation enzymes (Figueiredo et al., 2021; von Berlepsch et al., 2012), AAS is commonly deleted in engineered strains to prevent the reincorporation of FFA into lipids and promote FFA secretion. However, the physiological role of AAS in cyanobacteria under different conditions remains underexplored, including its potential contribution to membrane lipid remodeling through acyl chain recycling. Therefore, we sought to quantify reduced acyl-ACPs and acyl-ACP intermediates to assess changes in lipid metabolism due to variations in temperature and/or loss of AAS expression.

Previously, we developed a method (Nam et al., 2020; Jenkins et al., 2021) based on trichloroacetic acid (TCA) extraction to quantify acyl-ACPs from oleaginous plant tissues. However, applying this method to non-oleaginous systems, including plant leaves (Xu et al., 2023), resulted in fewer sensitively detected ACPs. Here, we developed an efficient method to characterize less-abundant acyl-ACPs from bacteria using anion exchange chromatography (AEX). The technique was combined with omics analysis to examine the adjustments in fatty acid metabolism that accompanied growth at different temperatures. We investigated the effects in wild-type *E. coli* and both wild-type and Δ*aas* mutant strains of *Picosynechococcus* sp. PCC 7002 (PCC 7002). PCC 7002 is a particularly important strain for the metabolic engineering community due to its potential for biotechnological applications and production of valued compounds, growth in variable conditions and with short (2.6 h) doubling time in optimal conditions, overall productivity, and well-studied physiology (Ludwig and Bryant, 2012; Davies et al., 2014; Work et al., 2015; Hendry et al., 2016; Ruffing et al., 2016a; Gao et al., 2018; Selão et al., 2019; Kachel and Mack, 2020). By profiling acyl-ACP pools and integrating omics data, we show that lack of AAS expression results in altered levels of lipases and desaturases that mediate membrane remodeling in response to growth in cooler temperatures. Unexpectedly, unsaturated acyl-ACPs were detected in the Δ*aas* mutant, indicating that residual acyl activation persists through alternative enzymatic routes or pathways, a finding that could not be elucidated with other pathway analysis approaches that has ramifications for metabolic engineering-based production of fatty acids in microbes. These findings suggest the presence of compensatory mechanisms that may limit the effectiveness of metabolic engineering strategies designed to enhance FFA production in cyanobacterial hosts. The results describe acyl chain recycling as a part of lipid remodeling and highlight the potential of AEX-based acyl-ACP profiling as an approach for dissecting temperature-dependent fatty acid and lipid metabolism in biotechnologically relevant microbes.

2. Materials and methods

2.1. Chemicals and reagents

DEAE Sephadex^{Tm} A-25 was purchased from GE Healthcare. Disposable Polypropylene gravity flow columns, 6 mL (66.7 mm × 12.9 mm, 20 μm frit pore size), were obtained from Marvelgent Biosciences Inc. Urea (99–100 %) and Amicon Ultra centrifugal filters (3 kDa cut-off) used for protein concentration were obtained from Millipore Sigma. To make Na-acetate buffer, sodium acetate trihydrate and acetic acid were obtained from Calbiochem and Merck, respectively. *r*Asp-N for the enzymatic digestion of acyl-ACPs was acquired from Promega.

2.2. Synthesis of ^{15}N labeled Acyl-ACP for absolute quantification

^{15}N-labeled acyl-ACPs were synthesized using a previously described method (Nam et al., 2020; Jenkins et al., 2021). The reaction mixture contained the following components: 50 mM MOPS (pH 6.5), 4 mM TCEP, 100 μM ^{15}N-labeled apo-ACP, 500 μM acyl-CoA, 10 % DMSO, 1 % Tween 20, 10 mM $MgCl_2$, 10 mM $MnCl_2$, and 25 μM 4′-phosphopantetheinyl transferase (Sfp). The reactions were incubated for 2 h at 37 °C, 180 rpm. The labeled acyl-ACPs were washed three times and concentrated in 50 mM MOPS (pH 6.5) using Amicon Ultra centrifugal filters (3 kDa cut-off). The yield of each acyl-ACP standard was determined by 16.5 % (w/v) Tris-Tricine SDS-PAGE obtained from Bio-Rad and confirmed by LC-MS/MS.

2.3. Mass spectrometry analysis of acyl-ACPs

The *r*Asp-N digestion products of acyl-ACPs (the acyl-4-phosphopantetheine-DSL) were separated on a Supelco Discovery® Bio Wide Pore C18-3 column and analyzed using a Thermo TSQ Altis triple quadrupole LC–MS/MS system. The mass spectrometer was operated in positive mode, and the data were acquired in SRM mode to detect and quantify the acyl-4-phophopantetheine-DSL peptide based on the parameters of *m/z* of the transmitted parent ion and *m/z* of the monitored product ion previously reported (Nam et al., 2020; Jenkins et al., 2021). Full LC gradient, MS parameters, and instrument settings are provided in the Supporting Information (SI).

2.4. Optimization of cell lysis methods to effectively inhibit thioesterase

An *E. coli* (MG1655 *ΔfadD ΔaraBAD*) strain overexpressing *Umbellularia californica* thioesterase (*E. coli-Uc*TE) (Jindra et al., 2023) was used to test and optimize the cell lysis method, and ensure effective inhibition of any residual thioesterase (TE) activity. *E. coli-Uc*TE was cultured, induced, quenched with cold methanol, and processed using two distinct cell lysis methods.

Method (I): The cell pellets were resuspended in 7 M urea on ice, 50 mM Na-acetate buffer, pH 5.5, and bead-milled at 30 Hz/s for 5 min.

Method (II): The pellets were resuspended in 50 mM Na-acetate buffer pH 5.5 on ice, and boiled for either 5 or 10 min in hot water (95–100 °C) as described in the Results and Discussion, followed by bead-milling at 30 Hz/s for 5 min.

TE inhibition was evaluated by incubating crude protein extracts with ^{15}N-labeled C12:0-ACP, followed by *r*Asp-N digestion and LC–MS/MS analysis. Full experimental details are provided in the SI.

2.5. Development of an anion exchange chromatography (AEX) method to isolate acyl-ACPs

The AEX approach was developed on a gravity column. The column was packed with a 2 mL slurry of DEAE resin (prepared as a mixture with

a ratio of 75 % settled resin to 25 % 50 mM Na-acetate buffer, pH 5.5). Various NaCl concentrations (0, 50, 100, and 200 mM) in a solution of 7 M urea, 50 mM Na-acetate buffer at pH 5.5 were tested to determine the effect of salt concentration in the wash buffer on acyl-ACPs purification.

*E. coli-Uc*TE was grown as described above and utilized for AEX development. Approximately 10 mL of culture collected 5 h post-induction (OD_{600} ~ 3) was quenched with an equal volume of cold 60 % MeOH/water (−20 °C), then centrifuged at 4,500*g* for 10 min at 4 °C to collect the pellets. The pellets were resuspended in 500 μL of 50 mM Na-acetate buffer and boiled for 5 min. A mixture of 300 pmol individual ^{15}N-labeled acyl-ACPs (C4:0, C8:0, C16:0, and C18:1 (9)-ACP representing short, medium, and long-chain acyl-ACPs) was spiked into the sample, followed by the addition of approximately 400–500 mg of 0.5 mm glass beads. The cells were disrupted by bead beating at 30 Hz/s for 5 min. Crude protein was separated from the glass beads using a gravity flow column through centrifugation at 180*g* for 1 min, followed by three washes with 1 mL of 7 M urea in 50 mM Na-acetate buffer at pH 5.5. The flowthrough was then centrifuged at 17,800*g* for 30 min at 4 °C, and the crude supernatant was collected and loaded into a column pre-equilibrated with 5–10 column volumes (CV) (20–30 mL) of an equilibration buffer (7 M urea, 50 mM Na-acetate buffer, pH 5.5).

After loading, the sample was mixed with DEAE resins by inversion for 1 min, followed by a 30–60 min incubation at room temperature to allow the resin beads to repack. Following the incubation, the columns were washed with 5–10 CV (20–30 mL) of wash buffer with various concentrations of NaCl (0, 50, 100, and 200 mM) in a solution of 7 M urea, 50 mM Na-acetate buffer at pH 5.5, taking care not to disturb the resin bed. Subsequently, the acyl-ACPs were eluted with two rounds of 1.5 mL of elution buffer (1 M NaCl, 50 mM Na-acetate buffer, pH 5.5) using centrifugation at 180*g* for 2 min. The eluate volume was concentrated to 200 μL using a 3 kDa cut-off filter unit via centrifugation at 4,500*g* at 4 °C. A control reaction was performed to assess acyl-ACP loss during AEX purification. A solution containing 300 pmol each of ^{15}N-labeled C4:0, C8:0, C16:0, and C18:1 (9)-ACP standards was processed identically to the eluate from this point onward. The resulting 200 μL concentrate was precipitated with nine volumes of cold ethanol (−20 °C), followed by digestion of acyl-ACPs with *r*Asp-N and analysis via LC-MS/MS as described previously.

2.6. Culture conditions for analyzing the impact of growth temperature and the quantity of acyl-acyl-ACPs in microbes

E. coli DH5α (*fhuA2Δ(argF-lacZ)U169 phoA glnV44 Φ80Δ(lacZ)M15 gyrA 96 recA1 relA1 endA1 thi-1 hsdR17*) from NEB (Catalog #: C2987H) was cultivated in LB media at 30 °C and 37 °C with shaking at 180 rpm until reaching mid-log phase (OD_{600} of 0.5–0.8). The 25 mL cultures were then quenched with an equal volume of cold 60 % MeOH/water (−20 °C). Next, the cell pellets were collected by centrifugation at 4,500*g* for 10 min at 4 °C, the supernatant was decanted, and the pellets were lyophilized and stored at −80 °C for acyl-ACPs analysis by the AEX method. Additionally, a chloroform-methanol extraction was performed following a previous report (Whaley et al., 2021), with modifications (see SI for method detail) to enhance the signal of the digested acyl-ACP products detected by mass spectrometry and to allow direct comparison with AEX purification.

The wild-type *Picosynechococcus* sp. PCC 7002 (wild-type PCC 7002) and the AAS-deficient strain (Δ*aas*) were cultivated in A+ media (Table S1) at 30 °C and 37 °C with shaking at 130 rpm, 1 % CO_2, 300 μmol/m^2/s illumination until reaching mid-log phase (OD_{730} of 0.6–0.7). Approximately 60 mL cultures were quenched with 90 mL volume of cold 30 % MeOH/water (−20 °C). The cell pellets were collected by centrifugation at 4,000*g* for 10 min at −4 °C, the supernatant was decanted, and the pellets were snap frozen with liquid nitrogen, lyophilized, and stored at −80 °C for acyl-ACPs analysis. Details of the construction and maintenance of the Δ*aas* strain are provided in the SI.

2.7. Isolation of acyl-ACPs using AEX to analyze the effect of growth temperature and the quantity of acyl-ACPs in microbes

The lyophilized *E. coli*, wild-type PCC 7002, and Δ*aas* PCC 7002 pellets were resuspended on ice in 500 μL of cold 50 mM Na-acetate buffer (pH 5.5) and transferred into a 2 mL tube on ice. Samples were boiled in a water bath for 5 min to inactivate the thioesterase. Subsequently, 20 pmol each of a^{15}N-labeled acyl-ACPs mixture (20 pmol each of C2:0, C4:0, C6:0, C8:0, C10:0, C12:0, C14:0, C16:0, C16:1 (9), C18:0, C18:1 (9), C18:2 (9,12), and C18:3 (9,12,15)-ACP and 80 pmol of holo-ACP) were added as internal standards for quantification and identification of acyl-ACPs present in the samples. Cells were bead-milled at 30 Hz/s for 5 min for disruption. Crude protein was separated from the glass beads using a column through centrifugation at 180*g* for 1 min, followed by three washes with 1 mL of equilibration buffer (7 M urea in 50 mM Na-acetate buffer at pH 5.5). The ~4 mL flowthrough was then centrifuged at 17,800*g* for 30 min at 4 °C, and the supernatant was collected and loaded onto a DEAE column with ~3 mL resin bed, pre-equilibrated with 5–10 CV (20–30 mL) of an equilibration buffer (7 M urea, 50 mM Na-acetate buffer, pH 5.5). After loading, the sample was mixed with DEAE resins by inverting for 1 min and then incubated for 30–60 min at room temperature. Following the 30–60 min incubation, the columns were washed with 5–10 CV (20–30 mL) of wash buffer (50 mM NaCl, 7 M urea, 50 mM Na-acetate buffer, pH 5.5) taking care not to disturb the resin bed, followed by elution with 3 mL of elution buffer (1 M NaCl, 50 mM Na-acetate buffer at pH 5.5) by centrifugation at 180*g* for 2 min. The eluate was processed as previously described for acyl-ACP analysis by HPLC-MS/MS.

2.8. Protein extraction, LC-MS proteomics analysis, and data processing

Lyophilized wild-type PCC 7002 and Δ*aas* pellets were extracted using the Thermo EasyPep MS Sample Prep Kit, digested, and analyzed by LC-MS/MS on a Dionex RSLCnano HPLC system coupled to an Orbitrap Fusion Lumos mass spectrometer. Peptides were separated on a PepMap C18 column using a 115-min gradient, and data were processed with Proteome Discoverer 2.4 against the *Picosynechococcus* sp. PCC 7002 UniProt database. Protein quantification was based on summed peptide intensities after curation. Full experimental details, including digestion, LC-MS conditions, database search parameters, and data processing workflow, are provided in the SI.

2.9. Statistics for the analysis of proteomics data

The data were normalized and Pareto-scaled in MetaboAnalyst 6.04[65] before being subjected to Partial Least Squares Discriminant Analysis (PLS-DA). Tukey's tests were performed in R version 4.4.0.

2.10. Lipid and fatty acid extraction and LC-MS lipidomics analysis

Lyophilized wild-type PCC 7002 and Δ*aas* pellets were extracted with cold methanol, spiked with isotopically labeled standards, and subjected to liquid–liquid extraction with MTBE. The resulting lipid fractions were resuspended in 2-propanol/MeOH containing internal standards and analyzed using a 1290 Infinity LC system coupled to a 6560 A IM-QTOF (Agilent). Lipids and fatty acids were separated on a Thermo Hypersil Gold C18 column with a 30-min gradient and detected in negative ion mode. LC–MS/MS was performed in iterative data-dependent acquisition (iDDA) mode. Full extraction protocol, LC conditions, and MS parameters are provided in the SI.

2.11. LC-MS processing and analysis of lipidomics data

LC-MS data processing, such as retention time alignment, molecular feature finding, and QA/QC evaluation, was performed using Progenesis QI (Waters Corporation, Manchester, UK). Tentative analyte

identifications were made implementing a mass measurement threshold of 15 ppm and 80 % isotopic envelope similarity and using various databases, including METLIN Metabolite and Chemical Entity Database, Human Metabolome Database, LIPID MAPS Structure Database, UCSD Metabolomics Workbench, and LipidBlast. LC-MS/MS iDDA analysis was performed in LipidAnnotator using a mass deviation threshold of 15 ppm.

2.12. Statistics for the analysis of lipidomic data

The processed LC-MS peak intensities were exported from Progenesis QI (Waters Corporation, Manchester, UK), normalized relative to the intensity of the $[M+Cl]^-$ ion of the internal standard (15:0–18:1 (d7)DG), Pareto-scaled in MetaboAnalyst 6.04 (Pang et al., 2024), and subjected to sPLS-DA using the MixOmics R package (Rohart et al., 2017). Tukey's tests were performed in R version 4.4.0.

3. Results and Discussion

3.1. Selection of AEX to purify microbial acyl-ACPs

ACP is a small acidic protein involved in fatty acid and polyketide biosynthesis (White et al., 2005; Buyachuihan et al., 2024). After synthesis as the inactive apo form, ACP is modified by adding a 4′-phosphopantetheine (Ppant) group at a conserved serine residue, forming holo-ACP (White et al., 2005; Buyachuihan et al., 2024). The free thiol group of Ppant on holo-ACP is a site for acyl groups to covalently attach to form an acyl-ACP (White et al., 2005; Buyachuihan et al., 2024). ACPs from different species have distinct isoelectric points (pI), as indicated by sequence analysis (Fig. 2A). Bacterial ACPs are highly acidic with pI values < 5.0 (Table S2). Previously, we developed a method to partially purify acyl-ACPs using TCA-based extraction (Nam et al., 2020; Jenkins et al., 2021). This method proved effective for plant seed studies where a significant amount of oil is produced (Morley et al., 2023), in high-oil tobacco leaves (Chu et al., 2022) and in an immortalized cell line (Kim et al., 2025); however, the technique lacked the sensitivity to measure the profile of acyl-ACPs from non-oleaginous microbes (Fig. S1). The lower pI and multiple negatively charged amino acid residues in the bacterial ACP (Fig. 2A and B) suggested that anion exchange chromatography (AEX) methods at low pH could facilitate the isolation of acyl-ACPs from complex protein samples and improve detection of acyl-ACPs from non-oleaginous microbes.

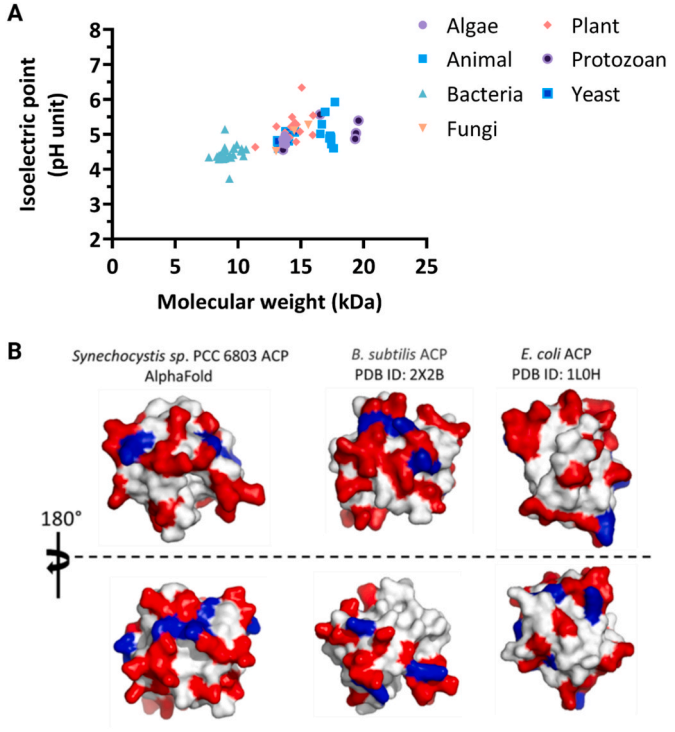

Fig. 2. (A) Isoelectric point (pI) vs. molecular weight of protein plots. The theoretical protein isoelectric points and protein molecular weights were computed from the proteins' amino acid sequences using the IPC2.0 web server (Kozlowski, 2021). **(B)** Surface plots of the acyl carrier protein (ACP) from *B. subtilis* (PDB 2 × 2B) (Martinez et al., 2010), *E. coli* (PDB 1L0H) (Roujeinikova et al., 2002), and *Synechocystis* sp. PCC 6803 (AlphaFold-Uniprot (UniProt, 2023)). ACP is anionic with a high content of negatively charged amino acids (indicated in red) and a low content of positively charged amino acids (indicated in blue), supporting the use of AEX for purification. Figures for the protein structures were generated using PyMOL.

3.2. Optimized cell lysis methods eliminate thioesterase activity and preserve acyl-ACP levels

One of the challenges in evaluating cellular FFA biosynthetic processes is the continued activity of thioesterases (TEs) that may not be adequately quenched during cell lysis and can result in artifacts. TEs catalyze the hydrolysis of thioesters, typically resulting in the formation of a free thiol and carboxylic acid. TEs cleave the thioester bond in acyl-ACP/CoA molecules, releasing FFA and ACP-SH/CoA-SH. To establish stringent conditions for inhibiting TE activity in whole-cell extracts, two cell lysis methods were evaluated using a TE activity assay. The assay included crude protein extracts incubated with ^{15}N-labeled C12:0-ACP, the canonical *Uc*TE substrate (Fig. 3A), as described in the methods section.

When treated with 7 M urea, *Uc*TE degraded 90 % of ^{15}N-labeled C12:0-ACP (i.e., Method I; Fig. 3B), indicating the urea did not effectively inhibit TE activity. When the cells were instead boiled, the *Uc*TE was completely inhibited (i.e., Method II; Fig. 3B) based on the similar peak areas of ^{15}N-labeled C12:0-ACP in the test sample and a control sample lacking TE. Furthermore, boiling samples for 5 or 10 min resulted in equally suitable inhibition of *Uc*TE activity (i.e., Method II; Fig. 3B). The combination of results suggested boiling is suitable for the isolation and quantification of acyl-ACPs. Other approaches including cold 60 % MeOH or high urea concentrations (e.g., 7 M) are commonly used to quench cellular metabolism or inhibit protein activity (Winder et al., 2008; de Koning and van Dam, 1992; Yang et al., 2018), although care must be taken to maintain the inactive TE state in whole cell extracts before AEX. It should be noted that fresh acyl-ACP standards are not impacted by the boiling process (Fig. S2), but the repeated freeze-thaw of standards followed by boiling can result in deterioration and negatively impact results.

3.3. Salt concentration modestly impacts AEX purification and detection of acyl-ACPs

The presence of NaCl in the equilibration buffer and wash buffers directly influenced the binding interaction between the acyl-ACPs and the DEAE Sepharose beads. Fine-tuning the concentration of NaCl in the buffers ensured the binding of acyl-ACP to the DEAE Sepharose beads while maximizing the removal of impurities during washing steps. By varying the concentration of NaCl (0, 50, 100, and 200 mM NaCl, see Materials and Methods for details) in buffer (7 M urea, 50 mM Na-acetate buffer, pH 5.5), we found that up to 50 mM NaCl can be included in the buffer without reducing the binding of spiked ^{15}N-labeled acyl-ACPs (C4:0, C8:0, C16:0, and C18:1 (9)-ACP) to DEAE Sepharose beads (Fig. S3A). In addition, 50 mM NaCl slightly improved the detection signal of some acyl-ACP species in *E. coli-Uc*TE samples (Fig. S3B). Thus, 50 mM NaCl was used in the wash buffer for subsequent experiments.

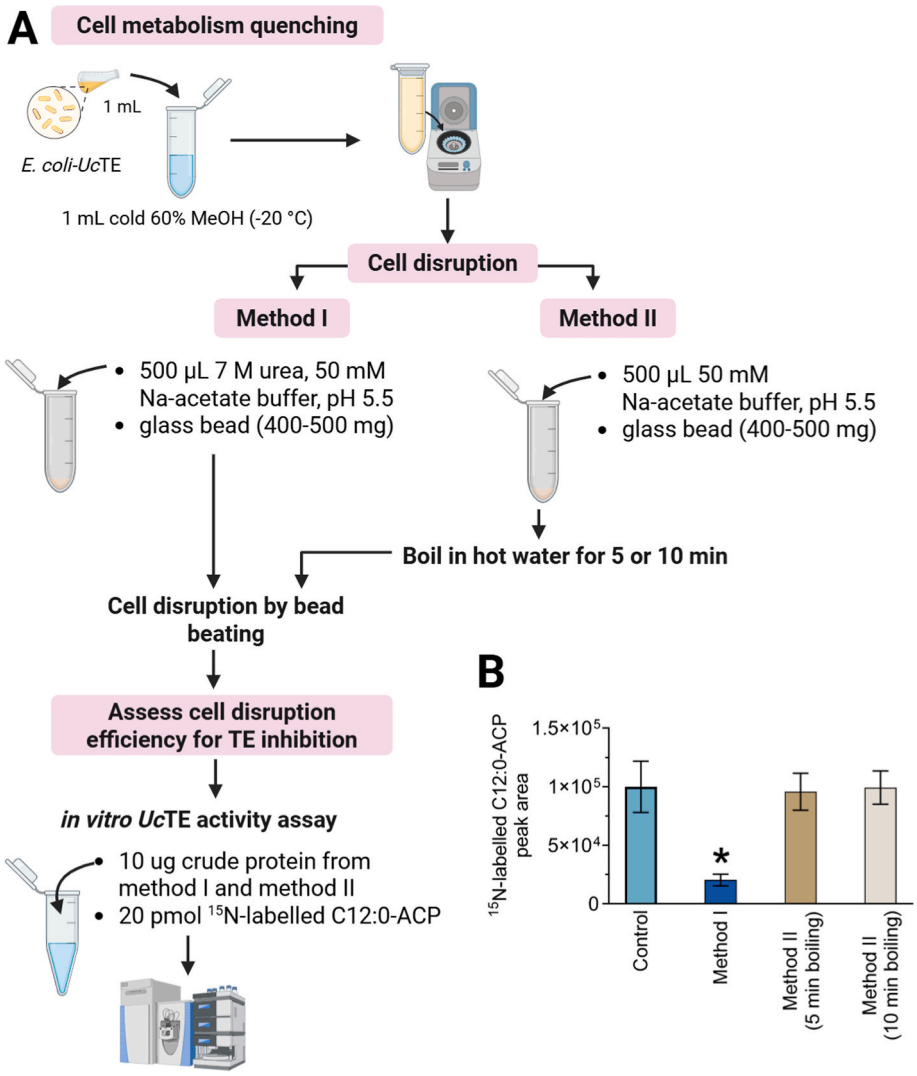

Fig. 3. Impact of cell lysis method on TE activity. (**A**) The experimental outline to determine the optimal cell lysis method for effectively inhibiting TE, an enzyme that catalyzes the cleavage of acyl-ACPs. *E. coli-Uc*TE was cultured, induced for overexpression, quenched with 60 % MeOH during harvesting, and lysed using two distinct approaches, as described in the Methods section. The effectiveness of each method in inhibiting TE activity was assessed using an *in vitro Uc*TE activity assay with crude protein extracts from Method I (7 M urea with bead milling) and Method II (heat treatment with bead milling). The extracts were incubated with ^{15}N-labeled C12:0-ACP at room temperature for 1 h in 50 mM sodium acetate buffer (pH 5.5), the buffer for optimizing the anion exchange chromatography method. (**B**) Comparison of the peak area of ^{15}N-labeled C12:0-ACP in the TE activity assay containing *Uc*TE, derived from cell lysis Methods I and II, with the control reaction (20 pmol of ^{15}N-labeled C12:0-ACP without 10 µg crude protein). Data are presented as mean ± SD., with n = 3. Asterisks (*) indicate significant differences compared to the control, as determined by Student's t-test ($p < 0.05$). Created with aid from BioRender.com.

3.4. AEX enables sensitive detection of temperature-dependent changes in acyl-ACP profiles and levels in E. coli

The AEX method was compared to other extraction strategies, including a chloroform-methanol ($CHCl_3$-MeOH) method (Fig. S4A and B) (see SI for method details). Using AEX, *E coli* acyl-ACPs and ACP intermediates were detected with greater sensitivity. Recovery analysis further showed that AEX achieved significantly higher acyl-ACP recovery across all acyl-ACP chain lengths than chloroform–methanol extraction (Fig. S5 and SI for method details), enabling more sensitive and comprehensive quantification of acyl-ACPs.

Small changes in temperature dramatically impact lipid acyl chain compositions. Such changes are necessary to maintain membrane fluidity. The remodeling of the lipids affects fatty acid biosynthesis and results in acyl chain recycling. We examined the adjustments in fatty acid composition that reflect the sensitive response through comparison of modest but significant temperature differences of 37 °C relative to 30 °C, then confirmed coarser details at 22 °C. As expected, acyl-ACP profiles changed with temperature, most notably the levels of unsaturated acyl-ACPs and corresponding ACP cycle intermediates that were elevated at 30 °C ($p < 0.05$, Fig. 4A and B). *E. coli* synthesizes unsaturated fatty acids via the oxygen-independent FabA-FabB pathway (Cronan and Thomas, 2009; Cronan, 2024; Cronan et al., 1969; Feng and Cronan, 2009; Zhang and Rock, 2008) (Fig. 4C). Cooler temperatures result in the production of more unsaturated fatty acids needed to maintain membrane fluidity (Cronan and Thomas, 2009; Birge and Vagelos, 1972; Cronan, 2024; Bloch, 1969; Kass et al., 1967; Cronan et al., 1969; Feng and Cronan, 2009; Norris and Bloch, 1963; Zhang and Rock, 2008; Hoogerland et al., 2024). Additionally, the measurement of acyl-ACP unsaturated intermediates provides metabolite-level confirmation of the desaturation cycle in *E. coli*, which has been mainly elucidated through biochemical activities (Cronan, 2024; Heath and Rock, 1996a; Yu et al., 2011b; Dodge et al., 2019).

The branch point between saturated and unsaturated fatty acid pathways in *E. coli* occurs at β-hydroxy-C10-ACP (Cronan and Thomas, 2009; Birge and Vagelos, 1972; Cronan, 2024; Bloch, 1969; Kass et al.,

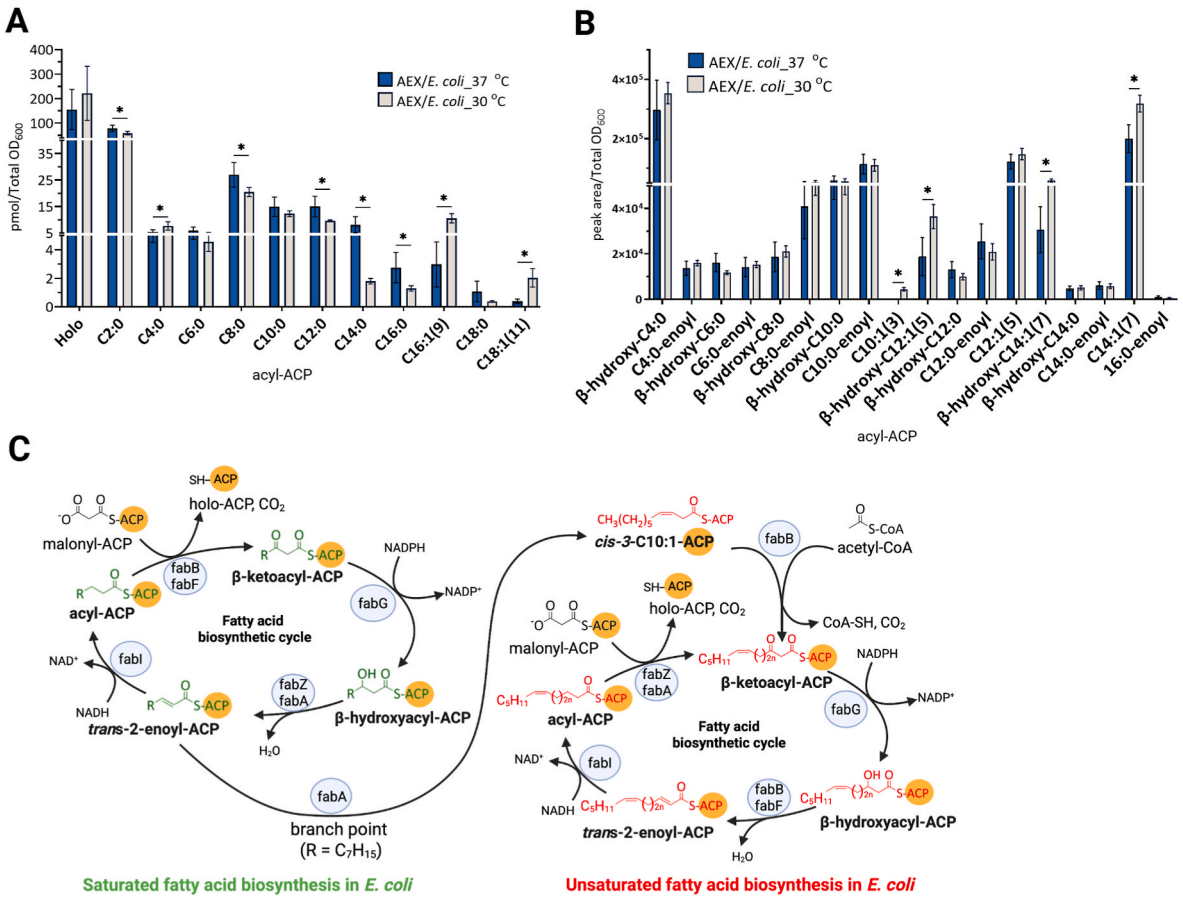

Fig. 4. Acyl-ACP levels under altered temperature in *E. coli*. (**A**) Reduced acyl-ACPs and (**B**) Levels of acyl-ACP intermediates in wild-type *E. coli* cultivated at 30 °C and 37 °C extracted using the AEX method. The pmol levels were obtained by comparison to corresponding ^{15}N-labeled acyl-ACP standards, except that C18:1-ACP quantification was based on a ^{15}N C18:1 (9) standard. In *E. coli*, C18:1 is naturally produced as C18:1 (11)-ACP (Birge and Vagelos, 1972; Bloch, 1969; Kass et al., 1967; Cronan et al., 1969; Feng and Cronan, 2009; Norris and Bloch, 1963). **(B)** The acyl-ACP intermediates were expressed as peak areas normalized to total OD_{600}. Data are presented as mean ± SD, n = 4 replicate cultures; asterisks denote significant differences by Student's t-test ($p < 0.05$). **(C)** The type II fatty acid biosynthesis pathway in *E. coli* (White et al., 2005; Birge and Vagelos, 1972; Cronan, 2024; Bloch, 1969; Kass et al., 1967; Cronan et al., 1969). Synthesis of saturated and unsaturated fatty acids is illustrated with green and red colors, respectively. Abbreviations: AccABCD—acetyl-CoA carboxylase; FabA—β-hydroxyacyl-ACP dehydratase/isomerase; FabB or FabF—β-ketoacyl-ACP synthase; FabD—malonyl CoA-ACP transacylase; FabG—β-ketoacyl-ACP reductase; FabH—β- ketoacyl-ACP synthase III; FabI—enoyl-ACP reductase; FabZ—β-hydroxyacyl-ACP dehydratase. Created with aid from BioRender.com.

1967; Cronan et al., 1969; Feng and Cronan, 2009; Norris and Bloch, 1963; Zhang and Rock, 2008), which can be converted to C10-enoyl-ACP via FabZ (Cronan et al., 1969) or *cis*-C10:1 (3)-ACP (i.e., C10:1 (3)-ACP) via FabA (Cronan et al., 1969), resulting in the synthesis of saturated and unsaturated fatty acids (Fig. 4C), respectively. We observed increased partitioning of β-hydroxy-C10-ACP into the unsaturated fatty acid pathway in response to lower temperatures including elevated levels of several intermediates and importantly unsaturates such as C10:1 (3)-ACP, C14:1 (7)-ACP, C16:1 (9)-ACP, and C18:1 (11)-ACP, in cells cultured at 30 °C ($p < 0.05$, Fig. 4A and B) which was further confirmed with additional experiments at 22 °C ($p < 0.05$, Fig. S6B). Conversely, saturated acyl-ACPs were lower ($p < 0.05$, Fig. 4A, B, S6A), indicating a temperature-sensitive metabolic valve involving FabI and FabB (Hoogerland et al., 2024) in *E. coli*.

3.5. Low temperature-induced accumulation of C16:1-ACP and C18:3-ACP in wild-type PCC 7002

With a sensitive method to investigate acyl-ACP metabolism established in *E. coli*, we inspected the impact of temperature on acyl-ACP profiles in the cyanobacterium PCC 7002 (Fig. 5A and B, S7), a fast-growing, genetically tractable strain that is biotechnologically relevant with established tools for gene editing, knockout, and overexpression (Ludwig and Bryant, 2012; Abernathy et al., 2019; Hendry et al., 2017; Bernstein et al., 2016; Ruffing, 2014; Ruffing et al., 2016b; Markley et al., 2015). PCC 7002 grown at 30 °C relative to 37 °C exhibited dramatically higher levels of saturated acyl-ACPs including C6:0, C8:0, C10:0, C12:0, C16:0, and C18:0-ACP and several unsaturated forms, C16:1-ACP and C18:3-ACP ($p < 0.05$, Tukey's test), while the levels of C18:1-ACP and C18:2-ACP were unchanged (Fig. 5A and B). These results were confirmed with a comparison at 22 °C ($p < 0.05$, Fig. S8).

The presence of unsaturated acyl-ACPs in cyanobacteria indicates a process whereby fatty acids were hydrolyzed from membrane lipids (Jimbo and Wada, 2022) and reactivated to acyl-ACPs by AAS (Fig. 5C), presuming that an unannotated acyl-ACP desaturase does not exist in cyanobacteria. We postulate that this cycle of lipid synthesis, desaturation, hydrolysis, and re-incorporation of acyl groups may increase the desaturation in membrane lipids, similar to plant-based acyl editing that cycles acyl chains on and off of phosphatidylcholine and results in highly polyunsaturated lipid compositions in oilseeds (Allen, 2016; Bates and Shockey, 2024; Zhou et al., 2019; Karki et al., 2019; Yang et al., 2017; Tjellström et al., 2011).

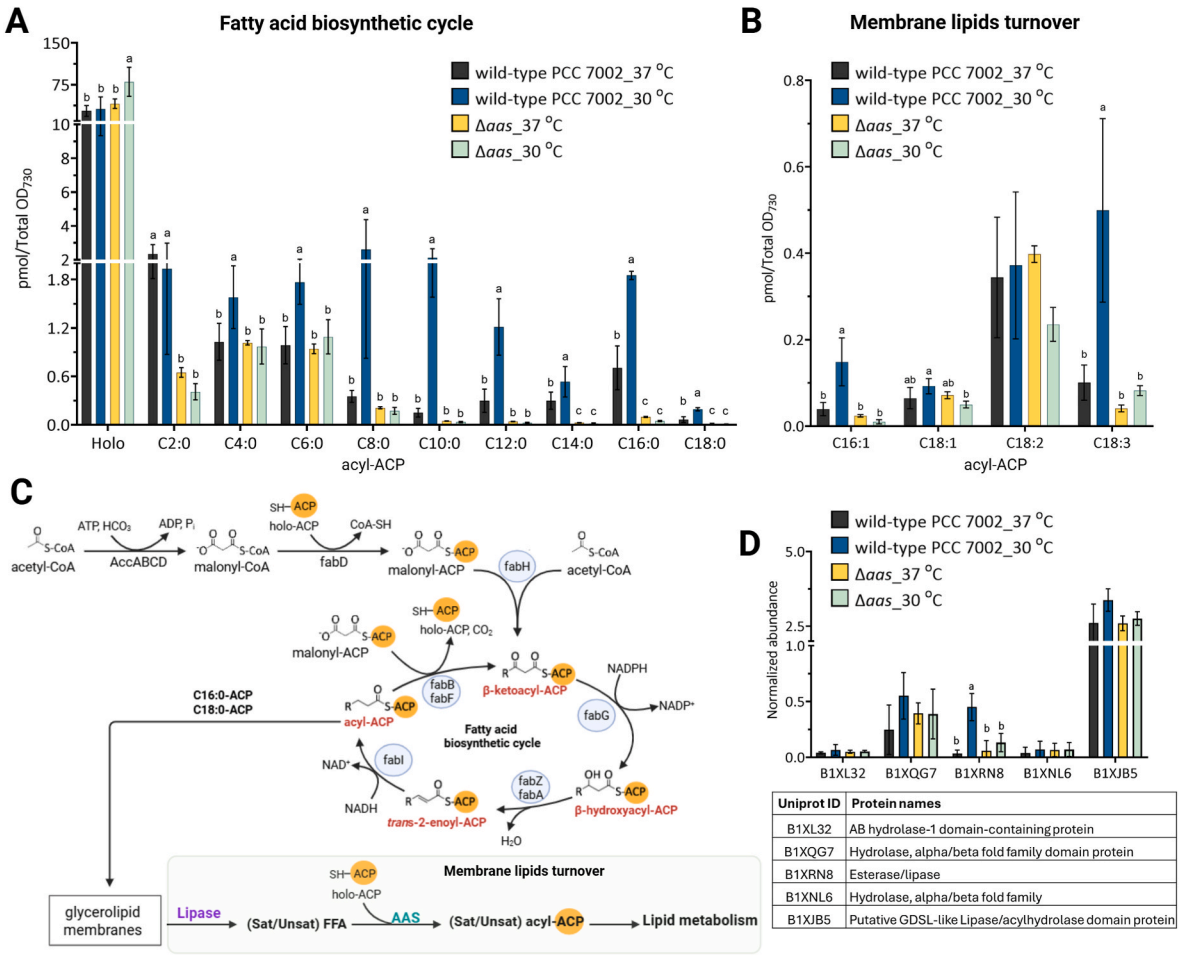

Uniprot ID	Protein names
B1XL32	AB hydrolase-1 domain-containing protein
B1XQG7	Hydrolase, alpha/beta fold family domain protein
B1XRN8	Esterase/lipase
B1XNL6	Hydrolase, alpha/beta fold family
B1XJB5	Putative GDSL-like Lipase/acylhydrolase domain protein

Fig. 5. Acyl-ACPs in wild-type PCC 7002 and the Δ*aas* strain cultivated at 30 °C and 37 °C. The quantification of the acyl-ACPs in (**A, B**) was achieved by comparison to the corresponding ^{15}N-labeled acyl-ACP internal standard. Data are presented as mean ± SD (n = 4 replicate cultures). Different letters indicate statistically significant differences ($p < 0.05$, Tukey's test) among groups. (**C**) Simplified type II fatty acid biosynthesis pathway and membrane lipid turnover in cyanobacteria (Sato et al., 2009). (**D**) Comparison level of protein annotated for hydrolase or esterases/lipases in the wild-type PCC 7002 and the Δ*aas* strain cultivated at 30 °C and 37 °C. The levels of individual proteins were expressed as peak areas normalized by the median, as described in the statistics section for proteomics data analysis in Materials and Methods. Data are presented as mean ± SD (n = 4 replicate cultures). Different letters indicate statistically significant differences ($p < 0.05$, Tukey's test) among groups. The absence of letters indicates no significant differences among groups. Abbreviations: AAS—acyl-acyl carrier protein synthetase; AccABCD—acetyl-CoA carboxylase; Des—desaturases; FabD—malonyl CoA-ACP transacylase; FabF—β-ketoacyl-ACP synthase; FabG—β-ketoacyl-ACP reductase; FabH—β- ketoacyl-ACP synthase III; FabI—enoyl-ACP reductase; FabZ—β-hydroxyacyl-ACP dehydratase; Sat—Unsaturated; Unsat—Unsaturated; FFA—free fatty acid. Created with aid from BioRender.com.

3.6. *Diminished AAS alters fatty acid synthesis and slows growth at lower temperature*

AAS plays an important role in recycling FFAs through esterification to holo-ACP (Kaczmarzyk and Fulda, 2010) that results in acyl-ACPs, which are substrates for lipid assembly. Unsaturated acyl-ACP species, particularly C16:1-ACP and C18:3-ACP, were elevated in PCC 7002 grown at 30 °C compared to 37 °C. Fatty acid synthesis in cyanobacteria does not include characterized acyl-ACP desaturases, although the biosynthesis of the monounsaturated form (C16:1-ACP) could be explained if a putative acyl-ACP desaturase were identified. Therefore, known plant acyl-ACP desaturase sequences (Schultz et al., 2000; Cahoon et al., 1992; Nishida et al., 1992; Nagai and Bloch, 1968) were used through a BLAST search to assess putative proteins in the PCC 7002 genome. There was little sequence similarity based on E-values, and no candidate proteins for an acyl-ACP desaturase were found (Table S3). Thus, the synthesis of C16:1 and C18:3-ACP is most likely the result of AAS-mediated activation of C16:1 and C18:3 FFA hydrolyzed from membrane lipids. Based on these observations, we investigated the role of AAS and its consequences on acyl-ACP profiles and membrane lipid homeostasis, using a PCC 7002 Δ*aas* strain.

Short to long chain acyl-ACPs involved in fatty acid synthesis (C4:0-ACP to C18:0-ACP) were less abundant in the Δ*aas* strain at both temperatures compared to the wild type, with a more pronounced reduction under low-temperature growth (Fig. 5A). Further, proteomics indicated enzymes involved in fatty acid biosynthesis, including AccA, AccC, AccD, FabH, FabZ, and FabI, were present at lower levels in the Δ*aas* strain at both temperatures (Fig. S9A). This reduction may reflect a cellular strategy to slow growth due to decreased carbon flow from the CO_2 fixation pathway (Forchhammer and Selim, 2020; Jahn et al., 2018; Battchikova et al., 2010), as proteins and enzymes in this process, along with those involved in nitrogen metabolism, were also reduced (Fig. S9B and C). Consistent with these findings, the growth rate of the Δ*aas* strain was lower than that of the wild type, with a more pronounced effect when the temperature was decreased to 22 °C (Fig. S10).

3.7. *Diminished AAS alters lipase induction at lower temperature*

Unexpectedly, we detected the presence of unsaturated acyl-ACPs, including C16:1, C18:1, C18:2, and C18:3-ACP, in both the wild-type

and *Δaas* strains (Fig. 5B–S8B).

We have previously reported (Nam et al., 2020) unsaturated acyl-ACPs in *Camelina sativa*, an oilseed, which were novel and remain somewhat enigmatic, but may also be related to changes in temperature. Because cyanobacteria are often polyploid, incomplete copies of the *aas* gene could exist and provide basal expression and activity; however, the *aas* gene and AAS protein were not detectable in the mutant line (Fig. S11A and B). Levels of the unsaturated acyl-ACPs in the Δ*aas* strain were comparable to the wild-type strain at 37 °C but were much lower than wild-type at 30 °C, indicating a diminished pool of cleaved unsaturated fatty acids available for reactivation. This result is consistent with a change in lipid remodeling, for example, the absence of lipase induction necessary to create the unsaturated acyl-ACP profile. Further, the presence of unsaturated acyl-ACPs when AAS is absent indicated alternative mechanisms capable of reactivating FFAs into acyl-ACPs that are responsive to temperature. The motif-based and functional enrichment analyses identified several candidate enzymes that may compensate for AAS loss (Figure S12 and S13A, B), providing potential targets for future functional characterization.

To assess changes in lipid remodeling, we analyzed proteins that could hydrolyze fatty acyl chains from membrane lipids (Fig. 5D). Esterases, lipases, and hydrolases were identified with B1XRN8, a putative esterase/lipase, elevated during low-temperature growth in wild-type PCC 7002 ($p < 0.05$, Tukey's test, Fig. 5D). In the mutant, the putative esterase/lipase remained unchanged and was lower than in the wild-type strain during low-temperature growth. Thus, combined proteomic and acyl-ACP results suggest that temperature-dependent membrane lipid remodeling is impaired in the Δ*aas* strain, due to reduced acyl-ACP availability and the absence of lipase induction under reduced temperature conditions.

3.8. Inactivation of AAS disrupts temperature-induced lipid desaturation and alters lipid remodeling

In cyanobacteria, increased membrane-bound desaturase activities (Los and Murata, 1998; Sato et al., 2009; Higashi and Murata, 1993; Wada et al., 1993a, 1993b; Effendi et al., 2023; Sakamoto et al., 1994; Starikov et al., 2022; Murata and Wada, 1995; Mendez-Perez et al., 2014) result in higher levels of unsaturated C16 and C18-containing glycerolipids (Sato et al., 2009; Sakamoto et al., 1997, 1998; Douchi et al., 2023). Lipidomic analysis of PCC 7002 indicated increases in select lipids, including MGDG 34:3 and SQDG 34:4 at 30 °C ($p < 0.05$, Tukey's test; Fig. 6A). The changes corresponded with elevated desaturase levels, including DesA (Δ12 desaturase) and DesB (ω3 desaturase). DesA showed a 4-fold induction ($p = 0.06$, Tukey's test) and DesB, a 12-fold induction ($p < 0.05$, Tukey's test) at 30 °C relative to 37 °C (Fig. 6B). The results matched observed increases in 16:0 and 18:0-ACP that are substrates for the 34-carbon unsaturated lipids. Although other lipid assembly intermediates, including DAG 32:3, were elevated, corresponding 32:3 galactolipids did not show a similar change. DGDG 32:3 decreased at the lower temperature, implying additional roles beyond membrane fluidity.

The Δ*aas* strain showed modestly impaired desaturation. MGDG 34:3 increased significantly at 30 °C, but the level of SQDG 34:4 did not

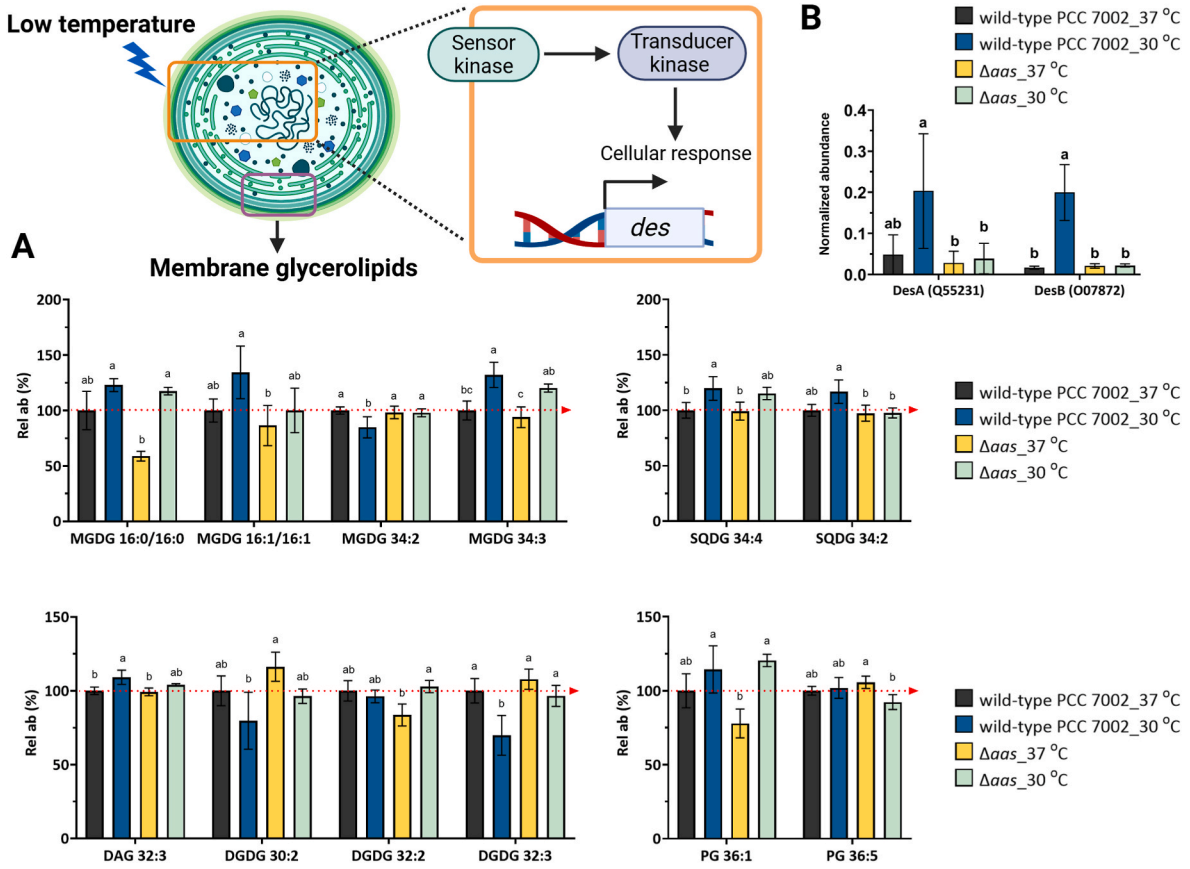

Fig. 6. Changes in lipid levels and proteins involved in the response to temperature changes in PCC 7002 and the Δ*aas* mutant. (**A**) Levels of lipid classes that changed significantly between wild-type PCC 7002 and the Δ*aas* strains. Levels are provided as relative abundance (Rel ab) to wild-type grown at 37 °C. Raw lipidomics data is available at the NIH Metabolomics Workbench, see Data Availability (**B**) Level of desaturase, DesA and DesB proteins in the wild-type PCC 7002 and the Δ*aas* strain cultivated at 30 °C and 37 °C. Protein peak areas were normalized by the median, as described in the methods. Data are presented as mean ± SD (n = 4 replicate cultures). Different letters indicate statistically significant differences ($p < 0.05$, Tukey's test) among groups, and the absence indicates no significance. Created with aid from BioRender.com.

change, consistent with the modest increase in 18:3-ACP (Fig. 5B). The levels of DesA and DesB remained unchanged between 30 °C and 37 °C in the Δ*aas* strain, at levels that were comparable to wild-type PCC 7002 at 37 °C. These findings indicate that the temperature-responsive regulation of desaturase proteins is impaired in the Δ*aas* strain and limits polyunsaturation when the temperature decreases. This may reflect an observed lower expression of two-component histidine kinases in the Δ*aas* strain that are known to influence desaturase expression (Mikami and Murata, 2003; Suzuki et al., 2000) (Fig. S14).

Other lipid patterns were comparable in the wild-type and Δ*aas* strains; however, there were several differences. At 30 °C, the Δ*aas* strain exhibited increased levels of MGDG 16:0/16:0 and phosphatidylglycerol (PG) 36:1 ($p < 0.05$) relative to the higher temperature. In the wild-type, these lipids did not change (Fig. 6). Thus, the absence of reduced temperature-induced desaturation through AAS-based lipid remodeling is accommodated by the elevation of saturated and monounsaturated lipids in a subset of molecular species in Δ*aas*.

4. Conclusion

In the current study, a sensitive anion exchange chromatography (AEX) approach to isolate and purify acyl-ACPs from microbes was developed and used to study temperature-dependent changes in acyl-ACP, fatty acid, and lipid biosynthesis. Microbial lipid metabolism in two important species, *E. coli* and *Picosynechococcus* sp. PCC 7002 was considered through the impact of acyl-ACP levels in response to the altered environment.

AEX enhanced the detection of long-chain acyl-ACPs and low-abundance intermediates compared to prior in-house methods (Nam et al., 2020; Jenkins et al., 2021), benefiting from acidic residues in microbial ACPs, which are retained on the column while impurities are removed through flow-through and salt elution. To further improve accurate quantification, we inhibited endogenous thioesterase activity by boiling the cell pellet, which preserved acyl-ACPs for analysis.

The method enabled the elucidation of acyl-ACP intermediates involved in saturated and unsaturated fatty acid biosynthesis, including elongation steps in *E. coli*, where intermediate levels changed in a temperature-dependent manner. Though the biochemical steps to create unsaturates in *E. coli* have been deduced using enzymology, our approach quantifies the intermediates involved in the pathway and therefore offers a unique strategy to assess important biochemical pathways for metabolic engineering and their perturbation under stress. The AEX method is readily applicable to acyl-ACP profiling in diverse microbial systems when the ACP pI is comparable to that of the organisms examined in this study (*E. coli* and cyanobacteria; ACP pI ≈ 4.0). In contrast, for target organisms with an ACP pI substantially higher than ~4.0 (e.g., yeast or plants), the working buffer pH should be adjusted to at least 0.5–1.0 units above the ACP pI to ensure efficient binding. Importantly, the buffer pH must remain within a range that is not excessively alkaline in order to preserve acyl-ACP integrity.

Temperature-dependent lipid metabolism in the cyanobacterium *Picosynechococcus* sp. PCC 7002 included changes in acyl-ACPs from fatty acid synthesis and lipid remodeling, and lipid desaturation. The acyl-ACP profile at lower temperatures suggested that Cyanobacteria recycle acyl chains from lipids, possibly to increase the degree of lipid desaturation. In the wild-type strain, acclimation to a limited reduction in temperature by 7 °C increased unsaturated glycerolipids such as MGDG and SQDG, accompanied by elevated levels of C16:1-ACP and C18:3-ACP, indicating lipid breakdown with desaturation processes mediated by DesA and DesB, and AAS activity. Recycling unsaturated acyl chains through the acyl-ACP mechanism may be a strategy to increase lipid desaturation, similar to acyl-editing in plants, but involving acyl-ACP instead of acyl-CoAs as substrates; however, this will require further study. In the Δ*aas* strain, the change in unsaturated glycerolipids due to a drop in temperature was limited and occurred without the induction of desaturases. However, the presence of polyunsaturated acyl-ACPs in the Δ*aas* strain suggested potential alternative compensatory mechanisms, such as the upregulation of acyltransferase enzymes, for which several candidates were identified from proteomic analysis. Given that engineering efforts to secrete fatty acids rely on an inactive AAS, the compensating mechanisms identified here present an unexplored opportunity to improve fatty acid yield in cyanobacterial production systems. These findings have fundamental and biotechnological implications for lipid metabolism and manipulation of fatty acid biosynthetic pathways to optimize the production of biofuels and other valuable bioproducts.

CRediT authorship contribution statement

Juthamas Jaroensuk: Writing – review & editing, Writing – original draft, Methodology, Investigation, Formal analysis, Data curation, Conceptualization. **Joshua P. Abraham:** Writing – review & editing, Investigation, Data curation. **Baltazar E. Zuniga:** Writing – review & editing, Investigation, Data curation. **Hawkins S. Shepard:** Writing – review & editing, Methodology, Investigation, Data curation. **Michael Wei:** Writing – review & editing, Methodology, Investigation, Data curation. **Russell Williams:** Writing – review & editing, Methodology, Investigation, Data curation. **Stewart A. Morley:** Writing – review & editing, Methodology, Investigation, Formal analysis, Data curation. **Maneesh Lingwan:** Writing – review & editing, Methodology, Investigation, Formal analysis, Data curation. **Jiahong Zhou:** Writing – review & editing, Methodology, Investigation, Formal analysis, Data curation. **Michael A. Jindra:** Writing – review & editing, Methodology. **Poonam Jyoti:** Writing – review & editing, Methodology, Investigation. **Bo Wang:** Writing – review & editing, Methodology. **Jody C. May:** Writing – review & editing, Methodology, Investigation. **John A. McLean:** Writing – review & editing, Resources, Project administration, Investigation, Funding acquisition, Conceptualization. **Jamey D. Young:** Writing – review & editing, Supervision, Resources, Project administration, Funding acquisition, Conceptualization. **Brian F. Pfleger:** Writing – review & editing, Supervision, Resources, Project administration, Funding acquisition, Conceptualization. **Doug K. Allen:** Writing – original draft, Supervision, Resources, Project administration, Methodology, Investigation, Funding acquisition, Formal analysis, Data curation, Conceptualization.

Declaration of competing interests

None.

Acknowledgements

The authors acknowledge the Donald Danforth Plant Science Center, including the Bioanalytical Chemistry Facility and the Subterranean Influences on Nitrogen and Carbon (SINC) Center, and the USDA-ARS. The lipidomics analysis utilized the resources of the Center for Innovative Technology at Vanderbilt University. In addition, this effort was supported by the Department of Energy Office of Science, Office of Biological and Environmental Research (BER) Award No. DE-SC0022207 and DE-SC0023142, National Science Foundation Award No. MCB-2242822, and the USDA National Institute of Food and Agriculture Grant No. 2023-67017-39419. The Orbitrap Fusion Lumos LC-MS/MS was acquired through the National Science Foundation Major Research Instrumentation grant (DBI-1827534). Drs. Rachel Combs-Giroir and Serena Hepkins are acknowledged for their suggestions for improving the manuscript.

Appendix A. Supplementary data

Supplementary data to this article can be found online at https://doi.org/10.1016/j.ymben.2025.11.004.

Data availability

Additional raw data files associated with this manuscript have been deposited at the NIH Metabolomics Workbench for lipidomics (10.21228/M88K07) and other mass spectrometry data for proteomics and acyl-ACP are deposited at Zenodo: 10.5281/zenodo.17547728, 10.5281/zenodo.17553702, and 10.5281/zenodo.17560020.

References

Abernathy, M.H., et al., 2019. Cyanobacterial carboxysome mutant analysis reveals the influence of enzyme compartmentalization on cellular metabolism and metabolic network rigidity. Metab. Eng. 54, 222–231. https://doi.org/10.1016/j.ymben.2019.04.010.

Allen, D.K., 2016. Assessing compartmentalized flux in lipid metabolism with isotopes. Biochim. Biophys. Acta Mol. Cell Biol. Lipids 1861, 1226–1242. https://doi.org/10.1016/j.bbalip.2016.03.017.

Allen, D.K., Bates, P.D., Tjellström, H., 2015. Tracking the metabolic pulse of plant lipid production with isotopic labeling and flux analyses: past, present and future. Prog. Lipid Res. 58, 97–120. https://doi.org/10.1016/j.plipres.2015.02.002.

Bates, P.D., Shockey, J., 2024. Towards rational control of seed oil composition: dissecting cellular organization and flux control of lipid metabolism. Plant Physiol. 197, kiae658. https://doi.org/10.1093/plphys/kiae658.

Bates, P.D., Ohlrogge, J.B., Pollard, M., 2007. Incorporation of newly synthesized fatty acids into cytosolic glycerolipids in pea leaves occurs via acyl editing. J. Biol. Chem. 282, 31206–31216. https://doi.org/10.1074/jbc.M705447200.

Bates, P.D., Durrett, T.P., Ohlrogge, J.B., Pollard, M., 2009. Analysis of acyl fluxes through multiple pathways of triacylglycerol synthesis in developing soybean embryos. Plant Physiol. 150, 55–72. https://doi.org/10.1104/pp.109.137737.

Battchikova, N., et al., 2010. Dynamic changes in the proteome of *Synechocystis* 6803 in response to CO(2) limitation revealed by quantitative proteomics. J. Proteome Res. 9, 5896–5912. https://doi.org/10.1021/pr100651w.

Bernstein, H.C., et al., 2016. Unlocking the constraints of cyanobacterial productivity: acclimations enabling ultrafast growth. mBio 7, e00949. https://doi.org/10.1128/mBio.00949-16, 00916.

Birge, C.H., Vagelos, P.R., 1972. Acyl carrier protein: XVII. Purification and properties of β-hydroxyacyl acyl carrier protein dehydrase. J. Biol. Chem. 247, 4930–4938. https://doi.org/10.1016/S0021-9258(19)44920-X.

Bloch, K., 1969. Enzymic synthesis of monounsaturated fatty acids. Acc. Chem. Res. 2, 193–202. https://doi.org/10.1021/ar50019a001.

Borgaro, J.G., Chang, A., Machutta, C.A., Zhang, X., Tonge, P.J., 2011. Substrate recognition by beta-ketoacyl-ACP synthases. Biochemistry 50, 10678–10686. https://doi.org/10.1021/bi201199x.

Buyachuihan, L., Stegemann, F., Grininger, M., 2024. How acyl carrier proteins (ACPs) direct fatty acid and polyketide biosynthesis. Angew. Chem. Int. Ed. 63, e202312476. https://doi.org/10.1002/anie.202312476.

Cahoon, E.B., Shanklin, J., Ohlrogge, J.B., 1992. Expression of a coriander desaturase results in petroselinic acid production in transgenic tobacco. Proc. Natl. Acad. Sci. U. S. A. 89, 11184–11188. https://doi.org/10.1073/pnas.89.23.11184.

Chan, David I., Vogel, Hans J., 2010. Current understanding of fatty acid biosynthesis and the acyl carrier protein. Biochem. J. 430, 1–19. https://doi.org/10.1042/bj20100462.

Chapman, K.D., Ohlrogge, J.B., 2012. Compartmentation of triacylglycerol accumulation in plants. J. Biol. Chem. 287, 2288–2294. https://doi.org/10.1074/jbc.R111.290072.

Choi, K.H., Heath, R.J., Rock, C.O., 2000. Beta-ketoacyl-acyl carrier protein synthase III (FabH) is a determining factor in branched-chain fatty acid biosynthesis. J. Bacteriol. 182, 365–370. https://doi.org/10.1128/JB.182.2.365-370.2000.

Chu, K.L., et al., 2022. Metabolic flux analysis of the non-transitory starch tradeoff for lipid production in mature tobacco leaves. Metab. Eng. 69, 231–248. https://doi.org/10.1016/j.ymben.2021.12.003.

Cronan, J.E., 2024. Unsaturated fatty acid synthesis in bacteria: mechanisms and regulation of canonical and remarkably noncanonical pathways. Biochimie 218, 137–151. https://doi.org/10.1016/j.biochi.2023.09.007.

Cronan, J.E., Thomas, J., 2009. Bacterial fatty acid synthesis and its relationships with polyketide synthetic pathways. Methods Enzymol. 459 (Part B), 395–433. https://doi.org/10.1016/S0076-6879(09)04617-5.

Cronan Jr., J.E., Birge, C.H., Vagelos, P.R., 1969. Evidence for two genes specifically involved in unsaturated fatty acid biosynthesis in *Escherichia coli*. J. Bacteriol. 100, 601–604. https://doi.org/10.1128/jb.100.2.601-604.1969.

Davies, F.K., Work, V.H., Beliaev, A.S., Posewitz, M.C., 2014. Engineering limonene and bisabolene production in wild type and a glycogen-deficient mutant of *Synechococcus* sp. PCC 7002. Front. Bioeng. Biotechnol. 2, 21. https://doi.org/10.3389/fbioe.2014.00021.

de Koning, W., van Dam, K., 1992. A method for the determination of changes of glycolytic metabolites in yeast on a subsecond time scale using extraction at neutral pH. Anal. Biochem. 204, 118–123. https://doi.org/10.1016/0003-2697(92)90149-2.

Dodge, G.J., et al., 2019. Structural and dynamical rationale for fatty acid unsaturation in *Escherichia coli*. Proc. Natl. Acad. Sci. U. S. A. 116, 6775–6783. https://doi.org/10.1073/pnas.1818686116.

Douchi, D., et al., 2023. Dryland endolithic *chroococcidiopsis* and temperate fresh water *Synechocystis* have distinct membrane lipid and photosynthesis acclimation strategies upon desiccation and temperature increase. Plant Cell Physiol. 65, 939–957 doi:10.1093/pcp/pcad139 %J Plant and Cell Physiology.

Effendi, D.B., Suzuki, I., Murata, N., Awai, K., 2023. DesC1 and DesC2, Δ9 fatty acid desaturases of filamentous cyanobacteria: essentiality and complementarity. Plant Cell Physiol. 65, 975–985. https://doi.org/10.1093/pcp/pcad153.

Faostat, F., 2022. Crops and livestock products. Statistics Division, Food and Agriculture Organization of the United Nations: Rome, Italy.

Feng, Y., Cronan, J.E., 2009. *Escherichia coli* unsaturated fatty acid synthesis: complex transcription of the fabA gene and in vivo identification of the essential reaction catalyzed by FabB. J. Biol. Chem. 284, 29526–29535. https://doi.org/10.1074/jbc.M109.023440.

Figueiredo, S.A.C., et al., 2021. Discovery of cyanobacterial natural products containing fatty acid residues. Angew. Chem. Int. Ed. 60, 10064–10072. https://doi.org/10.1002/anie.202015105.

Forchhammer, K., Selim, K.A., 2020. Carbon/nitrogen homeostasis control in Cyanobacteria. FEMS Microbiol. Rev. 44, 33–53. https://doi.org/10.1093/femsre/fuz025.

Gao, F., Wu, H., Zeng, M., Huang, M., Feng, G., 2018. Overproduction, purification, and characterization of nanosized polyphosphate bodies from *Synechococcus* sp. PCC 7002. Microb. Cell Fact. 17, 27. https://doi.org/10.1186/s12934-018-0870-6.

Heath, R.J., Rock, C.O., 1995. Enoyl-acyl carrier protein reductase (fabI) plays a determinant role in completing cycles of fatty acid elongation in *Escherichia coli*. J. Biol. Chem. 270, 26538–26542. https://doi.org/10.1074/jbc.270.44.26538.

Heath, R.J., Rock, C.O., 1996a. Inhibition of beta-ketoacyl-acyl carrier protein synthase III (FabH) by acyl-acyl carrier protein in *Escherichia coli*. J. Biol. Chem. 271, 10996–11000. https://doi.org/10.1074/jbc.271.18.10996.

Heath, R.J., Rock, C.O., 1996b. Roles of the FabA and FabZ beta-hydroxyacyl-acyl carrier protein dehydratases in *Escherichia coli* fatty acid biosynthesis. J. Biol. Chem. 271, 27795–27801. https://doi.org/10.1074/jbc.271.44.27795.

Hendry, J.I., Prasannan, C.B., Joshi, A., Dasgupta, S., Wangikar, P.P., 2016. Metabolic model of *Synechococcus* sp. PCC 7002: prediction of flux distribution and network modification for enhanced biofuel production. Bioresour. Technol. 213, 190–197. https://doi.org/10.1016/j.biortech.2016.02.128.

Hendry, J.I., et al., 2017. Rerouting of carbon flux in a glycogen mutant of Cyanobacteria assessed via isotopically non-stationary (13) C metabolic flux analysis. Biotechnol. Bioeng. 114, 2298–2308. https://doi.org/10.1002/bit.26350.

Higashi, S., Murata, N., 1993. An in vivo study of substrate specificities of acyl-lipid desaturases and acyltransferases in lipid synthesis in *Synechocystis* PCC 6803. Plant Physiol. 102, 1275–1278. https://doi.org/10.1104/pp.102.4.1275.

Hoogerland, L., et al., 2024. A temperature-sensitive metabolic valve and a transcriptional feedback loop drive rapid homeoviscous adaptation in *Escherichia coli*. Nat. Commun. 15, 9386. https://doi.org/10.1038/s41467-024-53677-5.

Intasian, P., et al., 2021. Enzymes, in vivo biocatalysis, and metabolic engineering for enabling a circular economy and sustainability. Chem. Rev. 121, 10367–10451. https://doi.org/10.1021/acs.chemrev.1c00121.

Jahn, M., et al., 2018. Growth of Cyanobacteria is constrained by the abundance of light and carbon assimilation proteins. Cell Rep. 25, 478–486.e478. https://doi.org/10.1016/j.celrep.2018.09.040.

Jaroensuk, J., et al., 2024. A versatile in situ cofactor enhancing system for meeting cellular demands for engineered metabolic pathways. J. Biol. Chem. 300, 105598. https://doi.org/10.1016/j.jbc.2023.105598.

Jenkins, L.M., Nam, J.-W., Evans, B.S., Allen, D.K., 2021. Quantification of acyl-acyl carrier proteins for fatty acid synthesisfatty acid synthesis using LC-MS/MS. Plant Lipids: Methods Protoc. 2295, 219–247. https://doi.org/10.1007/978-1-0716-1362-7_13.

Jimbo, H., Wada, H., 2022. Deacylation of galactolipids decomposes photosystem II dimers to enhance degradation of damaged D1 protein. Plant Physiol. 191, 87–95 doi:10.1093/plphys/kiac460 %J Plant Physiology.

Jindra, M.A., et al., 2023. Evaluation of strategies to narrow the product chain-length distribution of microbially synthesized free fatty acids. Metab. Eng. 77, 21–31. https://doi.org/10.1016/j.ymben.2023.02.012.

Jouhet, J., et al., 2024. Plant and algal lipidomes: analysis, composition, and their societal significance. Prog. Lipid Res. 96, 101290. https://doi.org/10.1016/j.plipres.2024.101290.

Kachel, B., Mack, M., 2020. Engineering of *Synechococcus* sp. strain PCC 7002 for the photoautotrophic production of light-sensitive riboflavin (vitamin B2). Metab. Eng. 62, 275–286. https://doi.org/10.1016/j.ymben.2020.09.010.

Kaczmarzyk, D., Fulda, M., 2010. Fatty acid activation in Cyanobacteria mediated by acyl-acyl carrier protein synthetase enables fatty acid recycling. Plant Physiol. 152, 1598–1610. https://doi.org/10.1104/pp.109.148007.

Karki, N., Johnson, B.S., Bates, P.D., 2019. Metabolically distinct pools of phosphatidylcholine are involved in trafficking of fatty acids out of and into the chloroplast for membrane production. Plant Cell 31, 2768–2788. https://doi.org/10.1105/tpc.19.00121.

Kass, L., Brock, D., Bloch, K., 1967. β-hydroxydecanoyl thioester dehydrase: I. Purification and properties. J. Biol. Chem. 242, 4418–4431. https://doi.org/10.1016/S0021-9258(18)99556-6.

Kim, D., et al., 2025. Mitochondrial NADPH fuels mitochondrial fatty acid synthesis and lipoylation to power oxidative metabolism. Nat. Cell Biol. 27, 790–800. https://doi.org/10.1038/s41556-025-01655-4.

Kozlowski, L.P., 2021. IPC 2.0: prediction of isoelectric point and pKa dissociation constants. Nucleic Acids Res. 49, W285–W292. https://doi.org/10.1093/nar/gkab295.

Lai, C.Y., Cronan, J.E., 2004. Isolation and characterization of beta-ketoacyl-acyl carrier protein reductase (fabG) mutants of *Escherichia coli* and *Salmonella enterica* serovar

Typhimurium. J. Bacteriol. 186, 1869–1878. https://doi.org/10.1128/JB.186.6.1869-1878.2004.
Li-Beisson, Y., Thelen, J.J., Fedosejevs, E., Harwood, J.L., 2019. The lipid biochemistry of eukaryotic algae. Prog. Lipid Res. 74, 31–68. https://doi.org/10.1016/j.plipres.2019.01.003.
Los, D.A., Murata, N., 1998. Structure and expression of fatty acid desaturases. Biochim. Biophys. Acta 1394, 3–15. https://doi.org/10.1016/s0005-2760(98)00091-5.
Los, D.A., Ray, M.K., Murata, N., 1997. Differences in the control of the temperature-dependent expression of four genes for desaturases in *Synechocystis* sp. PCC 6803. Mol. Microbiol. 25, 1167–1175. https://doi.org/10.1046/j.1365-2958.1997.5641912.x.
Lu, C., Napier, J.A., Clemente, T.E., Cahoon, E.B., 2011. New frontiers in oilseed biotechnology: meeting the global demand for vegetable oils for food, feed, biofuel, and industrial applications. Curr. Opin. Biotechnol. 22, 252–259. https://doi.org/10.1016/j.copbio.2010.11.006.
Ludwig, M., Bryant, D.A., 2012. *Synechococcus* sp. strain PCC 7002 transcriptome: acclimation to temperature, salinity, oxidative stress, and mixotrophic growth conditions. Front. Microbiol. 3, 354. https://doi.org/10.3389/fmicb.2012.00354.
Markley, A.L., Begemann, M.B., Clarke, R.E., Gordon, G.C., Pfleger, B.F., 2015. Synthetic biology toolbox for controlling gene expression in the cyanobacterium *Synechococcus* sp. strain PCC 7002. ACS Synth. Biol. 4, 595–603. https://doi.org/10.1021/sb500260k.
Martinez, M.A., et al., 2010. A novel role of malonyl-ACP in lipid homeostasis. Biochemistry 49, 3161–3167. https://doi.org/10.1021/bi100136n.
Mendez-Perez, D., Herman, N.A., Pfleger, B.F., 2014. A desaturase gene involved in the formation of 1,14-nonadecadiene in *Synechococcus sp*. strain PCC 7002. Appl. Environ. Microbiol. 80, 6073–6079. https://doi.org/10.1128/AEM.01615-14.
Mikami, K., Murata, N., 2003. Membrane fluidity and the perception of environmental signals in Cyanobacteria and plants. Prog. Lipid Res. 42, 527–543. https://doi.org/10.1016/s0163-7827(03)00036-5.
Morley, S.A., et al., 2023. Expression of malic enzyme reveals subcellular carbon partitioning for storage reserve production in soybeans. New Phytol. 239, 1834–1851. https://doi.org/10.1111/nph.18835.
Mukherjee, T., Kambhampati, S., Morley, S.A., Durrett, T.P., Allen, D.K., 2024. Metabolic flux analysis to increase oil in seeds. Plant Physiol. 197, kiae595. https://doi.org/10.1093/plphys/kiae595.
Murata, N., Wada, H., 1995. Acyl-lipid desaturases and their importance in the tolerance and acclimatization to cold of Cyanobacteria. Biochem. J. 308 (Pt 1), 1–8. https://doi.org/10.1042/bj3080001.
Murata, N., Wada, H., Gombos, Z., 1992. Modes of fatty-acid desaturation in Cyanobacteria. Plant Cell Physiol. 33, 933–941. https://doi.org/10.1093/oxfordjournals.pcp.a078344.
Nagai, J., Bloch, K., 1968. Enzymatic desaturation of stearyl acyl carrier protein. J. Biol. Chem. 243, 4626–4633. https://doi.org/10.1016/S0021-9258(18)93235-7.
Nam, J.W., et al., 2020. A general method for quantification and discovery of acyl groups attached to acyl carrier proteins in fatty acid metabolism using LC-MS/MS. Plant Cell 32, 820–832. https://doi.org/10.1105/tpc.19.00954.
Nishida, I., Beppu, T., Matsuo, T., Murata, N., 1992. Nucleotide sequence of a cDNA clone encoding a precursor to stearoyl-(acyl-carrier-protein) desaturase from spinach, *Spinacia oleracea*. Plant Mol. Biol. 19, 711–713. https://doi.org/10.1007/bf00026799.
Norris, A.T., Bloch, K., 1963. On the mechanism of the enzymatic synthesis of unsaturated fatty acids in *Escherichia coli*. J. Biol. Chem. 238, 3133–3134. https://doi.org/10.1016/S0021-9258(18)51880-9.
Pang, Z., et al., 2024. MetaboAnalyst 6.0: towards a unified platform for metabolomics data processing, analysis and interpretation. Nucleic Acids Res. 52, W398–W406. https://doi.org/10.1093/nar/gkae253.
Rohart, F., Gautier, B., Singh, A., Le Cao, K.A., 2017. mixOmics: an R package for 'omics feature selection and multiple data integration. PLoS Comput. Biol. 13, e1005752. https://doi.org/10.1371/journal.pcbi.1005752.
Roujeinikova, A., et al., 2002. X-ray crystallographic studies on butyryl-ACP reveal flexibility of the structure around a putative acyl chain binding site. Structure 10, 825–835. https://doi.org/10.1016/S0969-2126(02)00775-X.
Ruch, F.E., Vagelos, P.R., 1973. The isolation and general properties of *Escherichia coli* malonyl coenzyme A-acyl carrier protein transacylase. J. Biol. Chem. 248, 8086–8094. https://doi.org/10.1016/S0021-9258(19)43197-9.
Ruffing, A.M., 2014. Improved free fatty acid production in Cyanobacteria with *Synechococcus* sp. PCC 7002 as host. Front. Bioeng. Biotechnol. 2, 17. https://doi.org/10.3389/fbioe.2014.00017.
Ruffing, A.M., Jensen, T.J., Strickland, L.M., 2016a. Genetic tools for advancement of *Synechococcus* sp. PCC 7002 as a cyanobacterial chassis. Microb. Cell Fact. 15, 190. https://doi.org/10.1186/s12934-016-0584-6.
Ruffing, A.M., Jensen, T.J., Strickland, L.M., 2016b. Genetic tools for advancement of *Synechococcus* sp. PCC 7002 as a cyanobacterial chassis. Microb. Cell Fact. 15, 190. https://doi.org/10.1186/s12934-016-0584-6.
Sakamoto, T., Bryant, D.A., 1997. Temperature-regulated mRNA accumulation and stabilization for fatty acid desaturase genes in the cyanobacterium Synechococcus sp. strain PCC 7002. Mol. Microbiol. 23, 1281–1292. https://doi.org/10.1046/j.1365-2958.1997.3071676.x.
Sakamoto, T., Wada, H., Nishida, I., Ohmori, M., Murata, N., 1994. Delta 9 acyl-lipid desaturases of cyanobacteria. Molecular cloning and substrate specificities in terms of fatty acids, sn-positions, and polar head groups. J. Biol. Chem. 269, 25576–25580. https://doi.org/10.1016/S0021-9258(18)47288-2.
Sakamoto, T., Higashi, S., Wada, H., Murata, N., Bryant, D.A., 1997. Low-temperature-induced desaturation of fatty acids and expression of desaturase genes in the cyanobacterium *Synechococcus* sp. PCC 7002. FEMS Microbiol. Lett. 152, 313–320. https://doi.org/10.1111/j.1574-6968.1997.tb10445.x.
Sakamoto, T., Shen, G., Higashi, S., Murata, N., Bryant, D.A., 1998. Alteration of low-temperature susceptibility of the cyanobacterium *Synechococcus* sp. PCC 7002 by genetic manipulation of membrane lipid unsaturation. Arch. Microbiol. 169, 20–28. https://doi.org/10.1007/s002030050536.
Sato, N., Wada, H., 2009. In: Wada, Hajime, Murata, Norio (Eds.), Lipids in Photosynthesis: Essential and Regulatory Functions, 30. Springer Netherlands, pp. 157–177.
Schultz, D.J., Suh, M.C., Ohlrogge, J.B., 2000. Stearoyl-acyl carrier protein and unusual acyl-acyl carrier protein desaturase activities are differentially influenced by ferredoxin. Plant Physiol. 124, 681–692. https://doi.org/10.1104/pp.124.2.681.
Selão, T.T., Włodarczyk, A., Nixon, P.J., Norling, B., 2019. Growth and selection of the cyanobacterium *Synechococcus* sp. PCC 7002 using alternative nitrogen and phosphorus sources. Metab. Eng. 54, 255–263. https://doi.org/10.1016/j.ymben.2019.04.013.
Sérès, Y., et al., 2025. Decoupling of plastid and endomembrane homeoviscous response to low temperature and darkness in *Phaeodactylum tricornutum*. bioRxiv. https://doi.org/10.1101/2025.04.24.650388, 2025.2004.2024.650388.
Sohlenkamp, C., Geiger, O., 2015. Bacterial membrane lipids: diversity in structures and pathways. FEMS (Fed. Eur. Microbiol. Soc.) Microbiol. Rev. 40, 133–159. https://doi.org/10.1093/femsre/fuv008.
Starikov, A.Y., Sidorov, R.A., Goriainov, S.V., Los, D.A., 2022. Acyl-lipid Δ(6)-desaturase may act as a first FAD in Cyanobacteria. Biomolecules 12, 1795. https://doi.org/10.3390/biom12121795.
Suh, M.C., Uk Kim, H., Nakamura, Y., 2022. Plant lipids: trends and beyond. J. Exp. Bot. 73, 2715–2720. https://doi.org/10.1093/jxb/erac125.
Suzuki, I., Los, D.A., Kanesaki, Y., Mikami, K., Murata, N., 2000. The pathway for perception and transduction of low-temperature signals in *Synechocystis*. EMBO J. 19, 1327–1334. https://doi.org/10.1093/emboj/19.6.1327.
Tjellström, H., Yang, Z., Allen, D.K., Ohlrogge, J.B., 2011. Rapid kinetic labeling of arabidopsis cell suspension cultures: implications for models of lipid export from plastids. Plant Physiol. 158, 601–611. https://doi.org/10.1104/pp.111.186122.
UniProt, C., 2023. UniProt: the universal protein knowledgebase in 2023. Nucleic Acids Res. 51, D523–D531. https://doi.org/10.1093/nar/gkac1052.
von Berlepsch, S., et al., 2012. The acyl-acyl carrier protein synthetase from *Synechocystis* sp. PCC 6803 mediates fatty acid import. Plant Physiol. 159, 606–617. https://doi.org/10.1104/pp.112.195263.
Wada, H., Schmidt, H., Heinz, E., Murata, N., 1993a. In vitro ferredoxin-dependent desaturation of fatty acids in cyanobacterial thylakoid membranes. J. Bacteriol. 175, 544–547. https://doi.org/10.1128/jb.175.2.544-547.1993.
Wada, H., Avelange-Macherel, M.H., Murata, N., 1993b. The desA gene of the cyanobacterium *Synechocystis* sp. strain PCC 6803 is the structural gene for delta 12 desaturase. J. Bacteriol. 175, 6056–6058. https://doi.org/10.1128/jb.175.18.6056-6058.1993.
Whaley, S.G., Radka, C.D., Subramanian, C., Frank, M.W., Rock, C.O., 2021. Malonyl-acyl carrier protein decarboxylase activity promotes fatty acid and cell envelope biosynthesis in proteobacteria. J. Biol. Chem. 297, 101434. https://doi.org/10.1016/j.jbc.2021.101434.
White, S.W., Zheng, J., Zhang, Y.M., 2005. & Rock. The structural biology of type II fatty acid biosynthesis. Annu. Rev. Biochem. 74, 791–831. https://doi.org/10.1146/annurev.biochem.74.082803.133524.
Winder, C.L., et al., 2008. Global metabolic profiling of *Escherichia coli* cultures: an evaluation of methods for quenching and extraction of intracellular metabolites. Anal. Chem. 80, 2939–2948. https://doi.org/10.1021/ac7023409.
Work, V.H., et al., 2015. Lauric acid production in a glycogen-less strain of *Synechococcus* sp. PCC 7002. Front. Bioeng. Biotechnol. 3, 48. https://doi.org/10.3389/fbioe.2015.00048.
Xu, Y., et al., 2023. Arabidopsis acyl carrier protein 4 and RHOMBOID LIKE10 act independently in chloroplast phosphatidate synthesis. Plant Physiol. 193, 2661–2676. https://doi.org/10.1093/plphys/kiad483.
Yang, W., et al., 2017. Phospholipase Dζ enhances diacylglycerol flux into triacylglycerol. Plant Physiol. 174, 110–123. https://doi.org/10.1104/pp.17.00026.
Yang, Q., et al., 2018. Optimization of the quenching and extraction procedures for a metabolomic analysis of *Lactobacillus plantarum*. Anal. Biochem. 557, 62–68. https://doi.org/10.1016/j.ab.2017.12.005.
Yu, W.-L., et al., 2011a. Modifications of the metabolic pathways of lipid and triacylglycerol production in microalgae. Microb. Cell Fact. 10, 91. https://doi.org/10.1186/1475-2859-10-91.
Yu, X., Liu, T., Zhu, F., Khosla, C., 2011b. In vitro reconstitution and steady-state analysis of the fatty acid synthase from *Escherichia coli*. Proc. Natl. Acad. Sci. U. S. A. 108, 18643–18648. https://doi.org/10.1073/pnas.1110852108.
Yu, L., Zhou, C., Fan, J., Shanklin, J., Xu, C., 2021. Mechanisms and functions of membrane lipid remodeling in plants. Plant J. 107, 37–53. https://doi.org/10.1111/tpj.15273.
Zhang, Y.M., Rock, C.O., 2008. Membrane lipid homeostasis in bacteria. Nat. Rev. Microbiol. 6, 222–233. https://doi.org/10.1038/nrmicro1839.
Zhou, X.-R., et al., 2019. Reorganization of acyl flux through the lipid metabolic network in oil-accumulating tobacco leaves. Plant Physiol. 182, 739–755. https://doi.org/10.1104/pp.19.00667.